



Journal of Catalysis Vol. 272, Issue 2, 2010

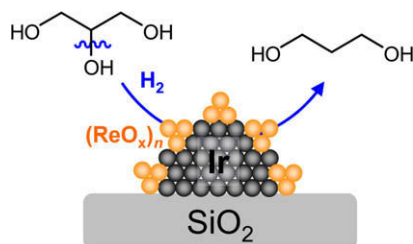
Contents

PRIORITY COMMUNICATION

Direct hydrogenolysis of glycerol into 1,3-propanediol over rhenium-modified iridium catalyst

pp 191–194

Yoshinao Nakagawa, Yasunori Shinmi, Shuichi Koso, Keiichi Tomishige*



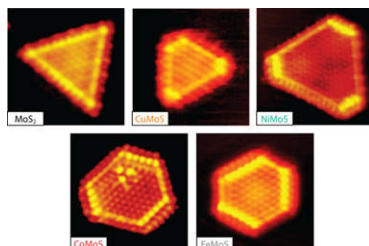
Silica-supported iridium particles modified with low-valent rhenium oxide clusters catalyze regioselective hydrogenolysis of glycerol to 1,3-propanediol in water.

REGULAR ARTICLES

Comparative atomic-scale analysis of promotional effects by late 3d-transition metals in MoS₂ hydrotreating catalysts

pp 195–203

Jakob Kibsgaard, Anders Tuxen, Kim G. Knudsen, Michael Brorson, Henrik Topsøe, Erik Lægsgaard, Jeppe V. Lauritsen*, Flemming Besenbacher

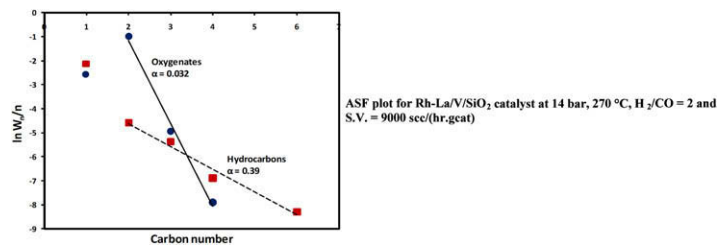


Using scanning tunneling microscopy (STM) and reactivity measurements, we determine a correlation between the atomic structure of transition metal-doped Me–Mo–S nanoclusters and the activity and selectivity in hydrotreating reactions.

La and/or V oxide promoted Rh/SiO₂ catalysts: Effect of temperature, H₂/CO ratio, space velocity, and pressure on ethanol selectivity from syngas

pp 204–209

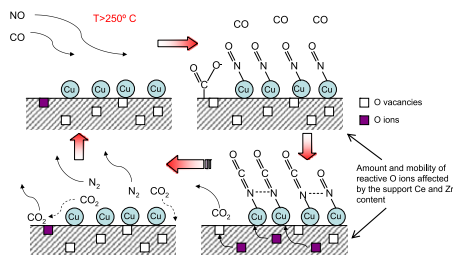
Nachal D. Subramanian, Jia Gao, Xunhua Mo, James G. Goodwin Jr., Walter Torres, James J. Spivey*

CO hydrogenation over La–V-oxide-promoted Rh/SiO₂ catalyst showed distinctly different chain growth factors (α) for oxygenates and hydrocarbons, suggesting that their formation either proceeds by different mechanisms or on different active sites.

Catalytic reduction of NO by CO over Cu/Ce_xZr_{1-x}O₂ prepared by flame synthesis

pp 210–219

Runduo Zhang*, Wey Yang Teoh, Rose Amal, Biaohua Chen, Serge Kaliaguine**

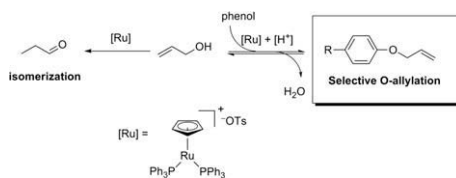


The catalytic reduction of NO by CO over flame-made Cu/Ce_xZr_{1-x}O₂ nanocomposites reveals two different rate controlling temperature-dependent *de*NO_x mechanisms: (1) Decomposition of N₂O by rapid activation of CO oxidation at low temperatures (150 °C < T < 250 °C) and (2) decomposition of organo nitrogen at T > 250 °C.

Remarkable activity of the isomerization catalyst [RuCp(PPh₃)₂](OTs) in O-allylation of phenol with allyl alcohol

pp 220–226

Jimmy A. van Rijn, Esther van Stapele, Elisabeth Bouwman*, Eite Drent

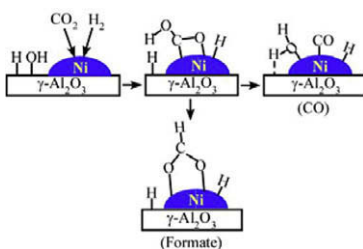


The highly active isomerization catalyst [RuCp(PPh₃)₂](OTs) changes its catalytic action to the selective O-allylation of phenols with allyl alcohol upon addition of a catalytic amount of a strong acid.

Effect of surface hydroxyls on selective CO₂ hydrogenation over Ni₄/γ-Al₂O₃: A density functional theory study

pp 227–234

Yun-xiang Pan, Chang-jun Liu*, Qingfeng Ge**

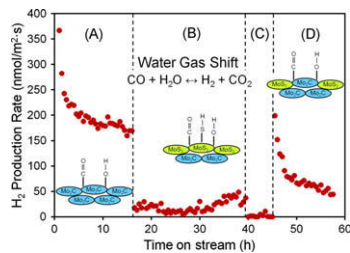


Hydroxylation of the γ-Al₂O₃ support alters the preference of CO₂ hydrogenation from formate to CO over the Ni/γ-Al₂O₃ catalyst.

Effects of sulfur on Mo₂C and Pt/Mo₂C catalysts: Water gas shift reaction

pp 235–245

Joshua A. Schaidle, Adam C. Lausche, Levi T. Thompson*

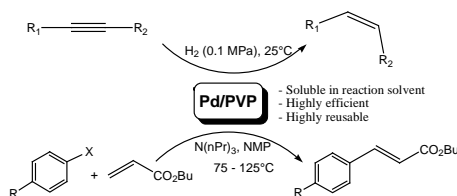


Sulfur exposure caused the Mo₂C surface to convert to MoS₂, which is moderately active for the water gas shift reaction. After re-carburization in 15% CH₄/H₂, the surface consisted of Mo₂C and MoS₂ domains.

New monodispersed palladium nanoparticles stabilized by poly-(N-vinyl-2-pyrrolidone): Preparation, structural study and catalytic properties

pp 246–252

Claudio Evangelisti*, Nicoletta Panziera, Aldo D'Alessio, Luca Bertinetti, Maria Botavina, Giovanni Vitulli

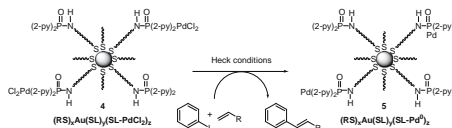


Monodispersed palladium nanoparticles stabilized by poly-(N-vinyl-2-pyrrolidone) were synthesized by metal vapour synthesis. Pd-PVP systems, dissolved in reaction solvent, show excellent catalytic activity and selectivity in the semi-hydrogenation of aliphatic alkynes and good activity in Mizoroki-Heck C-C coupling. The catalytic systems can be easily recovered and reused in further runs.

Preparation of a nonleaching, recoverable and recyclable palladium-complex catalyst for Heck coupling reactions by immobilization on Au nanoparticles

pp 253–261

Jun-Nan Young, Tsao-Ching Chang, Shih-Chung Tsai, Lin Yang, Shuchun Joyce Yu*

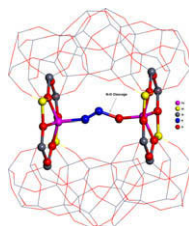


The partial palladation of the surface-supported spacer ligands on Au NPs affords a nonleaching hybrid system $(RS)_x\text{Au}(SL)_y(SL-PdCl_2)_z$ which is a highly efficient, quantitatively recoverable and effectively recyclable Heck catalyst.

N₂O decomposition over Fe-zeolites: Structure of the active sites and the origin of the distinct reactivity of Fe-ferrierite, Fe-ZSM-5, and Fe-beta. A combined periodic DFT and multispectral study

pp 262–274

Stepan Sklenak*, Prokopis C. Andrikopoulos, Bundet Boekfa, Bavornton Jansang, Jana Nováková, Lubomir Benco, Tomas Bucko, Juergen Hafner, Jiří Dědeček, Zdeněk Sobalík

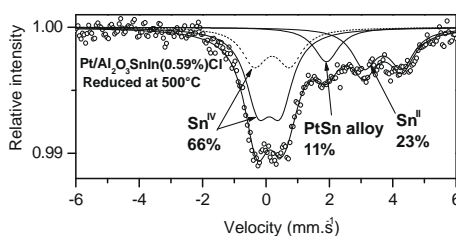


Two Fe(II) cations accommodated in two adjacent β sites of Fe-ferrierite form the active site responsible for the superior activity of Fe-ferrierite in the N_2O decomposition in the absence of NO.

Effect of indium in trimetallic Pt/Al₂O₃SnIn-Cl naphtha-reforming catalysts

pp 275–286

Ali Jahel, Priscilla Avenier, Sylvie Lacombe*, Josette Olivier-Fourcade, Jean-Claude Jumas

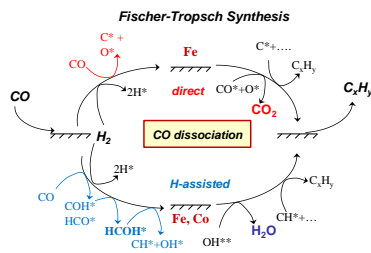


¹¹⁹Sn Mössbauer spectroscopy analysis revealed that addition of indium to bimetallic Pt/Al₂O₃Sn-Cl naphtha-reforming catalysts leads to stronger Pt-Sn interactions in the form of Pt_xSn alloys. Indium addition decreases the total conversion in the *n*-heptane dehydrocyclisation reaction and decreases hydrogenolysis selectivity.

CO activation pathways and the mechanism of Fischer–Tropsch synthesis

pp 287–297

Manuel Ojeda, Rahul Nabar, Anand U. Nilekar, Akio Ishikawa, Manos Mavrikakis*, Enrique Iglesia**

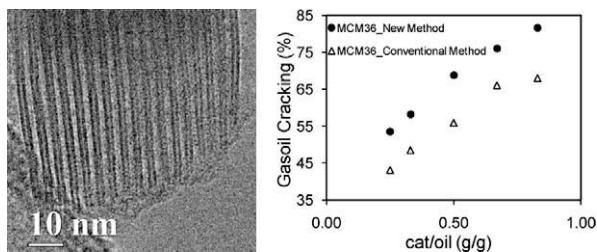


CO activation occurs predominantly by reaction with chemisorbed hydrogen before C–O bond cleavage with preferential rejection of oxygen as water on Fe and Co catalysts at conditions relevant to Fischer–Tropsch synthesis practice.

Influence of layer structure preservation on the catalytic properties of the pillared zeolite MCM-36

pp 298–308

Sudeep Maheshwari, Cristina Martínez, M. Teresa Portilla, Francisco J. Llopis, Avelino Corma*, Michael Tsapatsis**

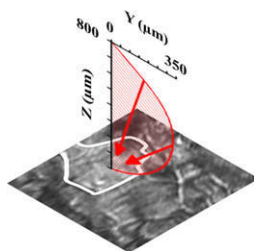


A method has been presented to prepare highly ordered MCM-36 materials without any structural destruction (see TEM). These pillared materials show higher catalytic activity compared to conventional MCM-36 materials.

Gas-phase coupling of reactive surfaces by oscillating reactant clouds

pp 309–314

Daniel Bilbao, Jochen Lauterbach*

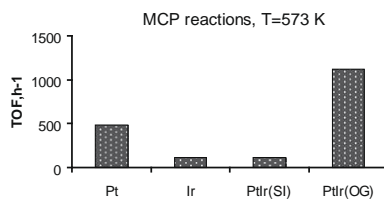


Angular CO uptake associated with kinetic oscillations on a single grain (outlined in white) of a polycrystalline Pt foil. Ultimately, the expanse of the CO adsorption distribution above a single grain will determine the spatial limits for the synchronization of activity on distant grains and in turn global catalyst performance ($p_{O_2} = 2.4 \times 10^{-3}$ mbar, $p_{CO} = 1.5 \times 10^{-4}$ mbar, $T = 534$ K).

Promising PtIr, catalysts for hydrocarbon transformation: Comparison of different preparation methods

pp 315–319

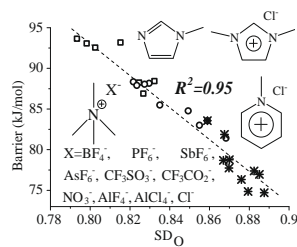
Christophe Poupin, Laurence Pirault-Roy, Camille La Fontaine, Lajos Tóth, Mounir Chamam, Attila Wootsch, Zoltán Paál*



PtIr/Al₂O₃ catalysts were prepared adding Ir by successive impregnation (SI) or by organometallic grafting (OG). The OG catalyst (with PtIr active sites) was most active in methylcyclopentane ring opening.

Theoretical study on the structure–reactivity relationships of acetylacetonate–Fe catalyst modified by ionic compound in C–H activation reaction pp 320–332

Xingbang Hu, Yong Sun, Jianyong Mao, Haoran Li*



The structure–reactivity relationships of 41 different acetylacetonate–Fe catalysts were summarized. Some effective modification methods to enhance the reactivity were proposed.